Theoretical Verification of Coulomb Order of Ions in a Storage Ring

Rainer W. Hasse
GSI Darmstadt, D-64291 Darmstadt, Germany
(Received 24 June 1999)

We verify theoretically that the anomalous longitudinal temperature reduction of strongly electron cooled heavy ions in the Experimental Storage Ring of GSI at very low density is explained by the fact that there is no intrabeam scattering and that the particles by their small relative velocity and their Coulomb repulsion cannot pass each other anymore. At the achievable momentum spreads, Coulomb order is reached at particle distances of the order of centimeters. It is also shown that under the given experimental conditions in the proton NAP-M experiment of 1980 intrabeam heating counteracts Coulomb order.

PACS numbers: 29.20.Dh, 29.27.Fh, 41.75.–i

In 1996, Steck *et al.* [1] reported on measurements with very low density and extremely electron cooled heavy ions in the Experimental Storage Ring (ESR) of GSI. By Schottky noise measurements they found a sharp drop of the longitudinal momentum spread $\delta p/p$ by an order of magnitude from 5×10^{-6} down to 5×10^{-7} for particle numbers from 10^3 down to 3 in the ring of about 100 m circumference. Thus, arranged in linear chains the average distances between the ions would be between 10 cm and 33 m. Because of magnetic field instability of the lattice $\delta p/p$ could not fall below this lower value. A typical example is shown in Fig. 1.

With a beam scraper the beam radius of the heavy beams could be determined to about 30 μm and by emittance measurements the transverse temperature was limited to about 1.5 eV. This anomaly resembles a strong suppression of intrabeam scattering below a certain threshold. Since heating of the beam is caused by intrabeam scattering, also the momentum spread is strongly inhibited, thus reaching the very low $\delta p/p \approx 5 \times 10^{-7}$.

It has been speculated that the final beam structures might be the storage ring analogs of Coulomb crystals as they were calculated in Ref. [2] and as they were found in ion traps [3]. In this Letter we confirm with the methods applied in Ref. [4] that indeed the beams resemble strings with particles which move slowly against each other in the beam direction, but, however, cannot pass at each other anymore. This type of order of a liquid caused by the nearest neighbors only we call Coulomb order in contrast to a Coulomb crystal which is generated by long range Coulomb interaction over many neighbors.

In order to explain this effect we perform classical Monte Carlo trajectory calculations of two charged particles heading at each other with constant focusing with the betatron frequency of the ESR and calculate the probability of these two particles being reflected at each other. It is sufficient to consider the interaction of two particles only since their mutual Coulomb repulsion acts only considerably at near distance of the order of tens of micrometers. Furthermore, it also suffices to apply the smooth approximation of constant focusing since the time periods of the lattice are much smaller than the collision times and, thus, are averaged over. Resonant instability caused by the lattice is unlikely to occur by the random nature of the positions of the few particles. To have a constant beam radius for all masses the experimental transverse temperature must obey the approximate relation $T_{\mathrm{trans}} = 7.5$ A meV. This energy is distributed among the two transverse degrees of freedom according to a Boltzmann distribution in harmonic potentials with equal betatron frequencies $\omega_\beta = 2\pi Q \beta c/L$, where βc is the beam velocity, $Q = 2.3$ is the average tune, and L is the circumference of the ring. The longitudinal kinetic energy is obtained from $M(c\beta\,\delta p/p)^2/(8\ln 2)$, where M is the mass; see Ref. [1].

In order to systematize the calculations, three dimensionless parameters are introduced: The relative transverse Θ_{trans} and longitudinal Θ_{long} kinetic energies measured in units of the mutual Coulomb energy of two particles at a distance d, $e_{\mathrm{C}} = q^2\gamma/d$, where q is the charge and γ is the relativistic parameter. These relative temperatures, thus, are the reciprocal gamma parameters in Wigner crystal theory; i.e., a one-component plasma is in the gaseous state for $\Gamma \ll 1$, in the liquid state for $1 < \Gamma < 100$, and

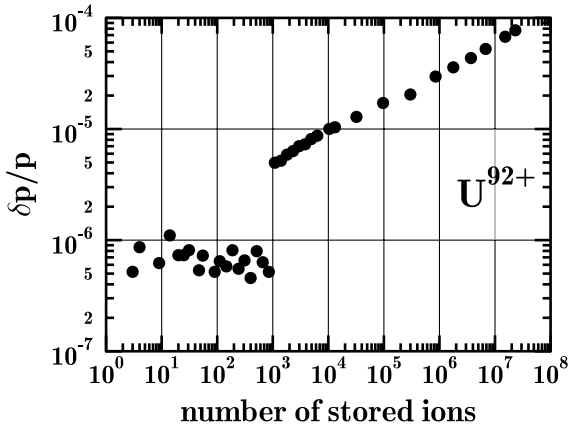

FIG. 1. Experimental momentum spread vs number of stored ions in the ESR for electron cooled U^{92+} ions at 240 MeV/u (from Ref. [1]).

 0031-9007/99/83(17)/3430(4)$15.00

in the crystalline state for $\Gamma \geq 170$. Note, however, that here Γ does not play a decisive role since distances involved are much larger than the Wigner-Seitz radius. Furthermore, the linear string density $\lambda = a_{\mathrm{WS}}/d$ is the axial number of particles within a Wigner-Seitz radius $a_{\mathrm{WS}} = (3q^2/2M\omega_\beta^2)^{1/3}$. Note that at zero temperature $\lambda = 0.709$ is the limiting value for a Coulomb string turning into a zigzag and $\lambda \approx 4$ would give a helix with a string at the center [2].

For typical experimental values of the kinetic energies a result is shown in Fig. 2. Within a factor of 2 in the distance, e.g., from 10 to 20 cm, the reflection probability rises sharply from 10% to 90%. On the other hand, Fig. 3 shows a contour plot of the reflection probability for fixed distance. Similarly, for given distance the reflection probability varies very slowly with Θ_{trans}; i.e., it goes from 10% to 90% about within a factor of 100 in Θ_{trans}, but more rapidly, with a factor of 5 only in Θ_{long}. As a rule of thumb $\Theta_{\mathrm{long}}\Theta_{\mathrm{trans}}^{1/3}$ stays constant for a given distance and fixed reflection probability. In the analysis of the experiments, hence, the results are little sensitive to the assumed transverse temperature of 7.5 A meV.

With the help of these tools the ESR experiments were analyzed with the results shown in Fig. 4. Here the lines of reflection probability (right scale) are calculated with the data of the last upper (open) experimental point. In all cases the calculated reflection probability rises sharply in the vicinity of this last hot data point thus indicating that for larger particle distances (or smaller particle densities) the ions cannot pass each other anymore. In the nickel and uranium frames the reflection probabilities are also calculated for the respective first ultracold data point (left lines). In the case of uranium it is shifted to smaller distances by almost 2 orders of magnitude. This indicates that here the ions move so slowly in the beam direction that reflection would happen even for much smaller interparticle distances which, however, cannot be reached experimentally. However, this distance is still 2 orders of magnitude larger than the Wigner-Seitz radius indicated by an arrow in Fig. 4 (the typical Coulomb crystal string distance) which means that real Coulomb crystals instead of Coulomb order only cannot be produced in the ESR with the present electron cooling methods and present lattice instabilities. An exception from this systematics is the case of argon which suggests that the last upper data point should be somewhat smaller than $\delta p/p = 4 \times 10^{-6}$. In the titanium data there is no drop in the momentum spread. The point used for evaluation evidently belongs already to the ultracold branch which can also be seen from the low longitudinal temperature of Table I.

A clear indication for the threshold behavior of intrabeam scattering can be seen in the nickel data. The first lower data points were recorded after a few ions got lost in the ring, thus increasing the average ion distance and jumping into the collisionless regime. After another few ions were lost, by some heating disturbance the data continue on the hot branch until even small perturbations cannot invoke any more heating, thus remaining on the lower branch. The smooth time evolution of the experimental noise power can be found in Ref. [1]. In this case the two calculated reflection probabilities are at threshold in this range of interparticle distances.

A summary of the data and of the results is shown in Table I. The linear density λ is about 5000 times smaller than the critical string density which shows again that the order reached is far from the one of Coulomb crystals. The average transverse rms displacement in the next to last column was calculated with [4] $\rho_{\mathrm{rms}} = d\sqrt{4\lambda^3\Theta_{\mathrm{trans}}/3}$. As assumed, it settles around 30 μm for all elements as noted by the authors of Ref. [1]. In the last column is shown the ratio of collisional time to betatron period of a particle, $\tau_{\mathrm{coll}}/\tau_\beta = \sqrt{T_{\mathrm{trans}}/T_{\mathrm{long}}} \times d/\rho_{\mathrm{rms}}$. As a result, thousands of betatron oscillations are performed during one binary collision, thus indicating that intrabeam scattering is negligible.

The two italicized lines are predictions for a proton experiment in the ESR storage ring with the energy of the NAP-M experiment [5] and for a future krypton

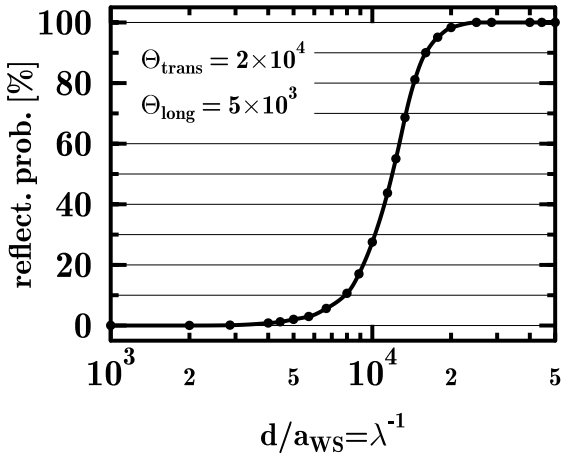

FIG. 2. Calculated reflection probabilities vs average distance between particles for given temperatures.

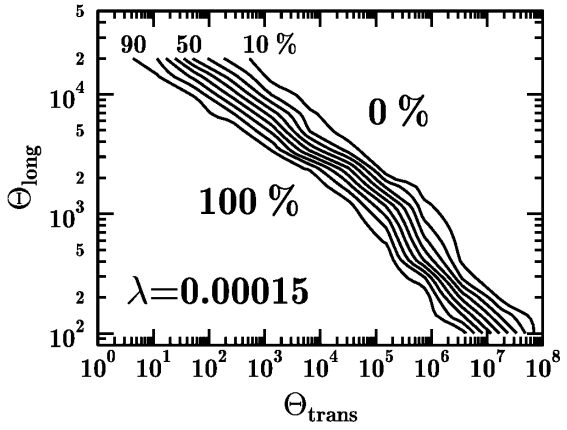

FIG. 3. Contour plot of the calculated reflection probabilities vs relative transverse and longitudinal temperature at fixed density $\lambda = 0.000\,15$.

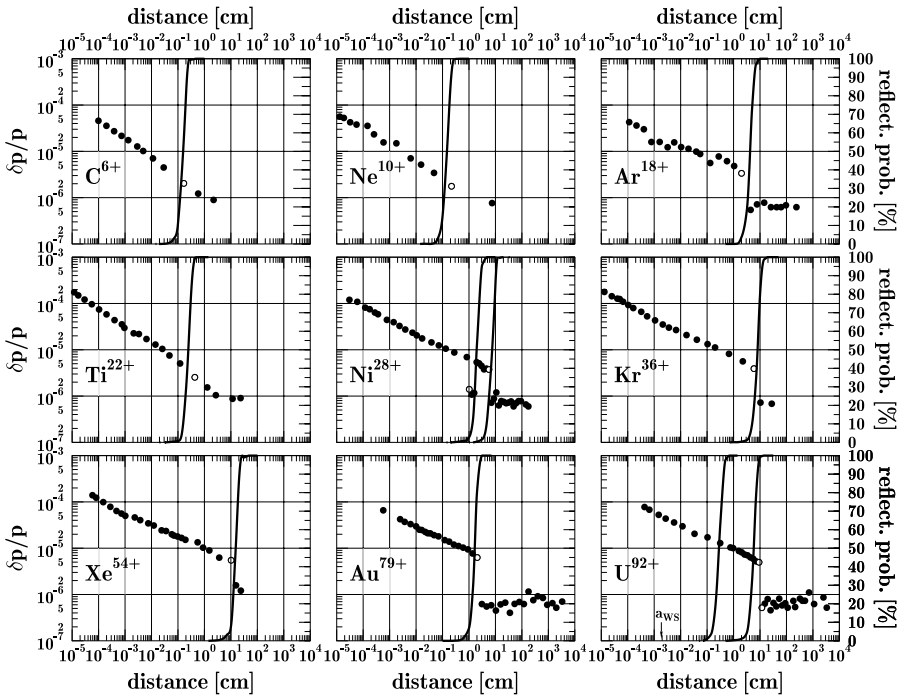

FIG. 4. Experimental momentum spreads (points, left scale) and calculated reflection probabilities (lines, right scale) vs average distance between ions for the various ESR experiments [1]. Reflection probabilities are calculated at the last upper open data point. In cases of two lines (nickel and uranium) the left lines are calculated for the first lower (ultracold) data point.

experiment in the synchroton SIS at GSI at injection energy with the recently installed electron cooler, respectively. The proton prediction is very close to the existing carbon data. On the other hand, due to the stronger focusing forces in the SIS (the horizontal and vertical tunes are 4.3 and 3.3, respectively) the threshold of 50% reflection will be shifted to larger linear densities closer to the critical string density, i.e., to smaller interparticle distances. Coulomb order can be reached with even larger momentum spreads with a maximum of 10^{-5}. Here the calculation of the reflection probability was carried out with anisotropic focusing, however, with little change in the results as compared to isotropic focusing.

Finally we analyze the cooling experiment with protons in the then existing Novosibirsk NAP-M storage ring [5]. This experiment could not be repeated. Here the authors suggested long ago that order has been reached. Their argument was based on the fact that if the proton current fell below 10 μA the noise power dropped to unmeasurable levels and thereafter stayed constant.

With the given data of circumference 47.25 m, average tune 1.29, energy 65 MeV, the number of particles in the ring for 10 μA current was $N = 2.5 \times 10^7$ from the relation $I_p = eNf_{\rm rev}$, where $f_{\rm rev}$ is the revolution frequency. An average transverse kinetic energy of 25 meV was derived from the measured beam radius of 100 μm

TABLE I. Experimental data, momentum spread $\delta p/p$, distance d, Wigner-Seitz radius $a_{\rm WS}$, linear density λ, longitudinal and transverse kinetic energies $T_{\rm long}$, $T_{\rm trans}$, reflection probability (rp), rms radius $\rho_{\rm rms}$, and ratio of collision time to betatron period. The entries apply to the last upper open data point of Fig. 4. The italicized lines are predictions.

Ring	Ion	E (MeV/u)	$\delta p/p$ (10^{-6})	d (cm)	$a_{\rm WS}$ (μm)	λ	$T_{\rm long}$ (meV)	$T_{\rm trans}$ (meV)	rp (%)	$\rho_{\rm rms}$ (μm)	$\tau_{\rm coll}/\tau_\beta$
ESR	$^{12}C^{6+}$	240	2	0.17	7.7	0.0046	1.5	90	68	30	450
ESR	$^{20}Ne^{10+}$	240	2	0.25	9.1	0.0036	0.40	170	80	30	700
ESR	$^{40}Ar^{18+}$	360	4	4	8.9	0.000 20	19	300	5	21	8500
ESR	$^{48}Ti^{22+}$	240	2.5	0	11.5	0.0026	9	370	100	30	950
ESR	$^{58}Ni^{28+}$	205	4	8	13.6	0.000 16	26	440	24	33	1300
ESR	$^{86}Kr^{36+}$	240	4	6	13.3	0.000 22	39	640	25	30	8000
ESR	$^{132}Xe^{54+}$	240	6	10	15.0	0.000 15	120	1000	10	30	10 000
ESR	$^{197}Au^{79+}$	360	6	2	14.0	0.000 70	290	1500	82	21	2200
ESR	$^{238}U^{92+}$	360	5	10	14.6	0.000 15	240	1800	99	21	13 000
ESR	*p*	*65*	*1*	*0.2*	*9.1*	*0.0045*	*0.01*	*7.5*	*50*	*70*	*1000*
SIS	*$^{86}Kr^{36+}$*	*11.4*	*15*	*0.5–10*	*50*	*0.004–0.01*	*40*	*90–200*	*50*	*60–90*	*100–4000*
NAP-M	*p*	65	1	2 μm	8.0	4.2	0.01	25	⋯	150	0.6

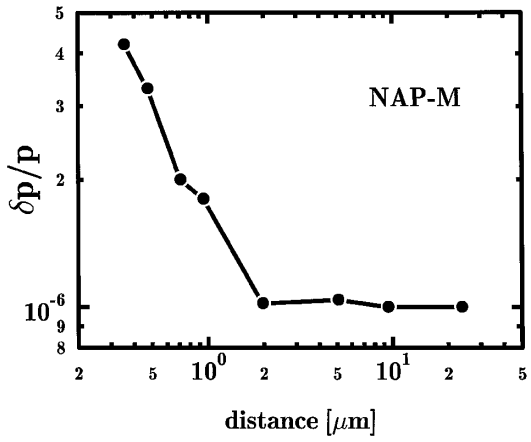

FIG. 5. Momentum spread vs average longitudinal distance between protons of the NAP-M experiment (after Ref. [5]).

and an average longitudinal kinetic energy of 10^{-4} eV was obtained from Schottky noise measurements. From this one gets the momentum spread of Fig. 5 with a critical $\delta p/p = 10^{-6}$.

According to the last row of Table I the linear density is $\lambda \approx 4$, indicating that the system is no longer in the linear regime and the average *axial* distance is 2 μm, much smaller than the Wigner-Seitz radius of 8 μm. The average *spatial* particle distance is about 40 μm. According to Table I, collision time and betatron period are about the same. Two particle calculations without taking into account other neighbors, hence, do not suffice to simulate this system. Therefore we performed full molecular dynamics calculations with periodic boundary conditions as in Ref. [4] with 1000 particles under constant focusing and computed the Coulomb interaction with Ewald summation [2].

Figure 6 shows the average over 20 simulations with random initial coordinates of the particles. With (short lower line) or without (long lower line) cooling, by intrabeam scattering after 200 betatron oscillations the longitudinal kinetic energy already reaches one-third of the value of the transverse kinetic energy. This yields an initial longitudinal heating rate of more than 50 eV/sec and after about 1000 betatron oscillations, i.e., about 400 μsec, without cooling thermal equilibrium ($\Theta_{\text{long}} = \frac{1}{2}\Theta_{\text{trans}}$) has been reached. Cooling with an e-folding time of 400 μsec has just the effect that the longitudinal temperature reaches with only half of the value of thermal equilibrium. This has to be compared with typical electron cooling times of a few milliseconds [6]. The authors' theory of collective interaction of the protons together with beam magnetization [7] may explain some suppression of intrabeam scattering in this case. However, it has not yet been applied to the data of the NAP-M experiment. Our predictions, on the other hand, cf. Table I, would yield Coulomb order for an interparticle distance of 0.2 cm, i.e., proton currents below 10 pA. Very similar conclusions on the existence of order in the NAP-M experiment have been drawn by Wei *et al.* [8].

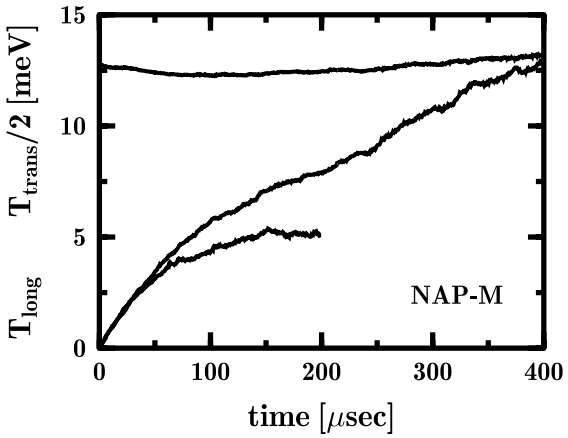

FIG. 6. Half transverse (upper curve) and increase of longitudinal kinetic energy (lower curves) due to intrabeam scattering up to thermal equilibrium ($T_{\text{long}} = \frac{1}{2}T_{\text{trans}}$) with the input data of the NAP-M experiment. Shown is the average over 20 Monte Carlo simulations. The long lower line is without cooling and the short one with cooling with e-folding time of 400 μsec.

In summary, our calculations of the reflection probabilities have shown that with the ESR experiments for the first time Coulomb order has been established in a heavy ion storage ring. This order is of liquid type where the particles still move slowly against each other but cannot pass anymore.

The author thanks M. Steck for valuable discussions.

[1] M. Steck, K. Beckert, H. Eickhoff, B. Franzke, F. Nolden, H. Reich, B. Schlitt, and T. Winkler, Phys. Rev. Lett. **77**, 3803 (1996); M. Steck, K. Beckert, H. Eickhoff, B. Franzke, F. Nolden, H. Reich, P. Spädtke, and T. Winkler, Hyperfine Interact. **99**, 245 (1996); M. Steck, Nucl. Phys. **A626**, 473c (1997).

[2] R. W. Hasse, and J. P. Schiffer, Ann. Phys. (N.Y.) **203**, 419 (1990).

[3] M. G. Raizen, J. M. Gilligan, J. C. Bergquist, W. M. Itano, and D. J. Wineland, J. Mod. Opt. **39**, 233 (1992); I. Waki, S. Kassner, G. Birkl, and H. Walther, Phys. Rev. Lett. **68**, 2007 (1992).

[4] R. W. Hasse, Phys. Rev. A **46**, 5189 (1992).

[5] E. N. Dementev, N. S. Dikansky, A. S. Medvedko, V. V. Parkhomchuk, and D. V. Pestrikov, Sov. Phys. Tech. Phys. **25**, 1001 (1980); G. I. Budker, N. S. Dikansky, V. I. Kudelainen, I. N. Meshkov, V. V. Parkhomchuk, D. V. Pestrikov, A. N. Skrinsky, and B. N. Sukhina, Part. Accel. **7**, 197 (1976).

[6] V. V. Parkhomchuk (private communication).

[7] V. V. Parkhomchuk, in *Proceedings of the Workshop on Electron Cooling and Related Applications: ECOOL 1984, Karlsruhe, Germany*, edited by H. Poth (Kernforschungszentrum Karlsruhe, Karlsruhe, 1984), p. 71; N. S. Dikansky and V. V. Parkhomchuk, *ibid.*, p. 275.

[8] J. Wei, A. Draeseke, A. M. Sessler, and X.-P. Li, in *Proceedings of the Eloisatron Workshop on Crystalline Beams, Erice, 1995*, edited by D. M. Maletić and A. G. Ruggiero (World Scientific, Singapore, 1996), p. 229.